

Zn and Cr abundances in damped Lyman alpha systems from the CORALS survey ^{*}

Chris J. Akerman¹, Sara L. Ellison², Max Pettini¹, and Charles C. Steidel³

¹ Institute of Astronomy, University of Cambridge, Madingley Road, Cambridge, CB3 0HA, UK. e-mail: cja@ast.cam.ac.uk, pettini@ast.cam.ac.uk

² University of Victoria, Dept. Physics & Astronomy, Elliot Building, 3800 Finnerty Road Victoria, V8P 1A1, British Columbia, Canada. e-mail: sarae@uvic.ca

³ Palomar Observatory, California Institute of Technology, MS 105-24, Pasadena, CA 91125, USA e-mail: ccs@astro.caltech.edu

Received / Accepted

Abstract. We present metal abundances in 15 damped Ly α systems (DLAs) from the Complete Optical and Radio Absorption Line System (CORALS) survey, designed to be free from any biasing effects due to extinction of QSOs by dust in intervening absorbers. It has long been suggested that such biasing may explain differences in metallicity between damped Ly α systems and coeval luminous galaxies, and between model predictions and observations. We use our measured zinc and chromium abundances (combined with those for five more CORALS DLAs from the literature, giving us a very nearly complete sample) to test whether the metallicity and degree of dust depletion in CORALS DLAs are significantly different from those of existing, larger, samples of DLAs drawn from magnitude limited, optical surveys. We find that the column density weighted metallicity of CORALS DLAs, $[\langle(\text{Zn}/\text{H})_{\text{DLA}}\rangle] = -0.88 \pm 0.21$ in the redshift interval $1.86 < z_{\text{abs}} < 3.45$, is only marginally higher than that of a control sample from the recent compilation by Kulkarni et al., $[\langle(\text{Zn}/\text{H})_{\text{DLA}}\rangle] = -1.09 \pm 0.10$. With the present limited statistics this difference is not highly significant. Furthermore, we find no evidence for increased dust depletions in CORALS DLAs—their $[\text{Cr}/\text{Zn}]$ ratios conform to the known trend of increasing depletion (decreasing $[\text{Cr}/\text{Zn}]$) with increasing metallicity, and we have encountered no cases where Cr is as depleted as in local cold interstellar clouds. These results, when combined with the earlier findings of the CORALS survey reported by Ellison et al. in 2001, make it difficult to invoke a dust-induced bias to explain the generally low level of chemical evolution exhibited by most DLAs. Rather, they indicate that large scale optical QSO surveys give a fair census of the population of high redshift absorbers.

Key words. galaxies: abundances – galaxies: evolution – ISM: dust, extinction – quasars: absorption lines

1. Introduction

Spectroscopic studies of absorption line systems along quasar sightlines are an important source of information regarding the chemical evolution history of neutral gas in the universe. Damped Ly α systems (DLAs, defined to have $N(\text{H I}) \geq 2 \times 10^{20}$ atoms cm^{-2} ; Wolfe et al. 1986), which make up the high column density end of the distribution of absorption line systems, are a particularly interesting subset of absorbers to study. They dominate the neutral

hydrogen content of the universe available for star formation up to $z \geq 4$ (e.g. Storrie-Lombardi & Wolfe 2000; Peroux et al. 2003) and are thought to be the progenitors of the disk galaxies we see today. DLAs have therefore been used as a tool for probing the evolution of galaxies, especially at high redshift where direct measurements are more difficult. Wolfe et al. (1995) found that the comoving mass density in neutral hydrogen in DLAs, Ω_{DLA} , is similar to the mass density in stars at redshift $z = 0$, and therefore proposed that its redshift evolution, $d\Omega_{\text{DLA}}/dz$, could be taken as a global measure of the rate at which gas in galaxies is converted into stars.

The metallicity evolution of galaxies has also been probed by chemical abundance measurements in DLAs (e.g. Pettini et al. 1997b, 1999; Prochaska & Wolfe 1999, 2000), which provide the most detailed information on the chemical composition of high- z galaxies. If indeed DLAs

^{*} This work is based in part on observations collected at the European Southern Observatory, Chile (ESO Nos. 69.A-0051A & 71.A-0067A) and at the W.M. Keck Observatory, which is operated as a scientific partnership among the California Institute of Technology, the University of California and the National Aeronautics and Space Administration. The Observatory was made possible by the generous financial support of the W.M. Keck Foundation.

are representative of the galaxy population at a given redshift, then one would expect that the evolution of their neutral hydrogen fraction and metallicity would track that of the general galaxy population as a whole. However, no strong evolution of either Ω_{DLA} or metallicity (Z_{DLA}) has been seen in studies from $z \sim 3.5$ down to $z \sim 0.5$ (e.g. Rao & Turnshek 2000; Ryan-Weber et al. 2003; Kulkarni et al. 2005).

Furthermore, it is now well established that DLAs are generally at the low end of the metallicity distribution of galaxies at redshifts $z = 2 - 3$ (see, for example, Figure 32 of Pettini 2004). The typical DLA metallicity at this epoch is only $Z_{\text{DLA}} \simeq -1.2$, or $\approx 1/15$ of solar (Pettini et al. 1999; Kulkarni et al. 2005), while near-solar metallicities are common for luminous galaxies detected directly in their rest-frame ultraviolet, optical, and far-infrared light (e.g. Pettini et al. 2002; Shapley et al. 2004; de Mello et al. 2004; Swinbank et al. 2005).

This difference could have a number of causes. Selecting galaxies through H I absorption may preferentially pick out chemically unevolved systems, either because galaxies with generally low rates of star formation dominate the cross-section (Mo, Mao & White 1998), or because the H I cross-section is largest during a stage prior to the onset of star formation. However, direct imaging of DLA galaxies shows a varied population of hosts which span a range of luminosities and morphological types (Boissier, Péroux, & Pettini 2003; Rao et al. 2003; Chen & Lanzetta 2003; Weatherley et al. 2005—see also Ryan-Weber et al. 2003). Abundance gradients may contribute to the difference in metallicity between the outer regions—which offer the larger cross-section for absorption—and the inner regions of galaxies where star formation activity is more prominent (Pettini et al. 1994a; Chen, Kennicutt, & Rauch 2005; Christensen et al. 2005; Ellison, Kewley, & Mallén-Ornelas 2005b). Quantitatively, however, the magnitude of such gradients has recently been questioned in nearby spirals (Bresolin, Garnett, & Kennicutt 2004), and remains unknown at high redshifts.

A third possibility is that damped Ly α systems which are both metal- and gas-rich do exist, but are systematically underrepresented in current samples drawn from magnitude-limited QSO surveys. The hypothesis is that even moderate amounts of dust associated with intervening galaxies may be sufficient to preferentially exclude reddened QSOs from optical surveys, and that the statistics of DLAs would accordingly be skewed by such bias against dusty absorbers. It is this third possibility which we address in the present paper.

The idea of dust obscuration of QSOs has a long history (e.g. Heisler & Ostriker 1988) and received observational support by the work of Pei, Fall, & Bechtold (1991) who found the spectra of QSOs with DLAs in the redshift range $1.77 \leq z_{\text{abs}} \leq 2.80$ to have statistically steeper continuum slopes than those of a control sample. On the basis of these results, Fall & Pei (1993) proposed that between 10% and 70% of bright QSOs at $z = 3$ may have been missing from optical samples. This claim is now tempered by

the recent re-analysis by Murphy & Liske (2004) based on the much larger compilation of QSO spectra made available by the Sloan Digital Sky Survey (SDSS—Stoughton et al. 2002). From the comparison of 70 QSOs lying behind DLAs at $2.0 < z_{\text{abs}} < 4.0$ with a control sample which is one order of magnitude larger, Murphy & Liske concluded that the difference in the continuum slopes α between the two sets of spectra is only $\Delta\alpha = -0.04 \pm 0.05$ (using the usual definition of the spectral index, whereby the QSO continuum flux is a power law of the form $f_{\nu} \propto \nu^{\alpha}$), corresponding to a limit on the colour excess due to SMC-like dust-reddening of $E(B-V) < 0.02 \text{ mag}$ (3σ). This value is significantly lower than $\Delta\alpha = -0.38 \pm 0.13$ reported by Pei et al. (1991). Similarly, Ellison, Hall & Lira (2005a) find $E(B-V) < 0.05 \text{ mag}$ (3σ) from a study of the optical to infrared colours of a subsample of CORALS QSOs with DLAs in the range $1.8 < z_{\text{abs}} < 3.5$.

However, the SDSS results still do not preclude the possibility that highly obscured QSOs may be missing, or underrepresented in optical samples (since SDSS QSOs are optically selected). Theoretically, such selection effects have been appealed to in order to reconcile the predictions of hydrodynamic simulations (Cen et al. 2003; Churches, Nelson & Edmunds 2004; Nagamine, Springel, & Hernquist 2004) and galactic chemical evolution models (Prantzos & Boissier 2000) with the observations. Observationally, their importance is suggested by the apparent anti-correlation between neutral hydrogen column density $N(\text{H I})$ and metallicity Z_{DLA} first pointed out by Boissé et al. (1998).

It is to assess quantitatively the importance of dust-induced bias for the statistics of DLAs that the Complete Optical and Radio Absorption Line System (CORALS) survey was originally conceived. As the name implies, this programme aims at measuring the properties of DLAs in a complete sample of QSOs selected at radio wavelengths, where dust obscuration is not expected to be an issue. In the first stage of the project, Ellison et al. (2001b) identified a sample of 22 DLAs from intermediate dispersion spectroscopy of all the QSOs (66) with emission redshift $z_{\text{em}} \geq 2.2$ in the Parkes quarter-Jansky sample of flat-spectrum radio sources (Jackson et al. 2002; Hook et al. 2003). The optical spectra were of sufficient quality to measure $N(\text{H I})$ in the 22 DLAs, enabling Ellison et al. (2001b) to determine both the number density of DLAs per unit redshift, $n(z)$, and the corresponding comoving mass density of neutral gas, Ω_{DLA} . The values found, $n(z) = 0.31_{-0.08}^{+0.09}$ and $\log \Omega_{\text{DLA}} = -2.59_{-0.24}^{+0.17}$ at a mean redshift $\langle z \rangle = 2.37$, are higher than the corresponding quantities previously determined from optically selected QSO samples, but only marginally so. In particular, the CORALS survey did not uncover a population of high column density ($N(\text{H I}) > 10^{21} \text{ cm}^{-2}$) DLAs in front of faint QSOs. Within the limitations imposed by the small size of their sample, Ellison et al. (2001b) concluded that selection effects due to intervening dust may at most account for an underestimate by a factor of ~ 2 in Ω_{DLA} .

The H I results alone, however, do not tell us about the metal and dust content of CORALS DLAs and whether they are higher, on average, than those of the optically selected DLAs which have been studied extensively over the last fifteen years. These are the questions which we explore in the present work.

Specifically, we have conducted a follow-up programme of high resolution spectroscopy of the CORALS DLAs aimed at measuring in particular the abundances of zinc and chromium. Meyer, Welty & York (1989) and Pettini, Boksenberg & Hunstead (1989, 1990) first drew attention to the diagnostic value of these two elements. Both are iron-peak elements, whose abundances track that of Fe to within ± 0.1 – 0.2 dex in Galactic stars of metallicities from solar to about 1/100 of solar (Chen, Nissen & Zhao 2004; Cayrel et al. 2004 and references therein). In the interstellar medium of the Milky Way, on the other hand, Zn is one of the few elements which show little affinity for dust grains, unlike Cr which is usually highly depleted (Savage & Sembach 1996). In combination, therefore, these two elements can be used to obtain approximate measures of the overall degree of metal enrichment, via the $[\text{Zn}/\text{H}]$ ratio, and the fraction of refractory elements locked up in solid form, via the $[\text{Cr}/\text{Zn}]$ ratio.¹ Both elements have absorption lines of their dominant ionisation stages in H I regions conveniently located at $\lambda\lambda 2026, 2062 \text{ \AA}$ (Zn II) and $\lambda\lambda 2056, 2062, 2066 \text{ \AA}$ (Cr II). All of these factors account for the fact that Zn II and Cr II absorption lines from DLAs have been the target of many studies since the 1990s, even though echelle spectrographs on 8-10 m class telescopes now afford a more comprehensive assessment of the overall chemical composition of QSO absorbers (e.g. Prochaska et al. 2001). Accordingly, in this paper we focus on the abundances of Zn and Cr in CORALS DLAs and compare them with the large body of such measurements now available for optically selected DLAs.

The paper is organised as follows. In §2 we describe the observations, data reduction process and column density measurements, while in §3 we list the abundances measured in the DLAs in our sample. We compare the CORALS Zn and Cr abundances to previous surveys in §4 and discuss our findings, together with our conclusions in §5.

2. Observations and Data Reduction

The CORALS sample of QSOs found to have DLAs with absorption redshifts $1.8 \leq z_{\text{abs}} \leq z_{\text{em}}$ consists of a total of 18 QSOs (22 DLAs; Ellison et al. 2001b). Prior to this study, spectra of sufficiently high resolution and signal-to-noise ratio (S/N) for abundance determinations had already been obtained (either by us or by others) for five of these DLAs and have appeared in the literature. We therefore describe here only observations made on the

remainder of the CORALS sample, details of which are collected in Table 1.

B-band magnitudes in column (2) have been taken from Table 2 of the recent study of Ellison et al. (2005a) except where indicated. Emission redshifts z_{em} in column (3) have been reproduced directly from Table 3 of Ellison et al. (2001b), while the values of DLA absorption redshift, z_{abs} listed in column (4) were determined from the observations presented here and are quoted to the precision of our measurements. One QSO from the CORALS sample, B1251–407, is too faint ($B = 23.7$) for high resolution spectroscopy and no abundance measurements are therefore available for the two DLAs identified by Ellison et al. in its spectrum. However, we do not expect this small gap in our survey to affect the conclusions of the present study for two reasons. First, the two DLAs in B1251–407 are at higher redshifts than the rest of the CORALS sample ($z_{\text{abs}} = 3.533$ and 3.752). Second, their neutral hydrogen column densities, $N(\text{H I}) = 4 \times 10^{20}$ and 2×10^{20} , are at the lower end of the DLA column density distribution. Thus, the metal and dust content of these two DLAs, even if they turned out to be significantly different from those of the rest of the sample, would have only a minor impact on integrated quantities such as the column density weighted metallicity considered in §4. Specifically, if we assume that, unlike most DLAs, these two systems have a solar abundance of Zn, the column density weighted mean metallicity of the CORALS sample would be increased by only 0.1 dex.

2.1. Data Acquisition

The observations were made between April 2002 and March 2004 during several runs on a range of telescopes and instruments. The majority of the data were obtained in service mode using the Ultraviolet and Visual Echelle Spectrograph (UVES; Dekker et al. 2000) on the European Southern Observatory Very Large Telescope (VLT). The spectra of B0405–331 and B0913+003 were obtained with the Echelle Spectrograph and Imager (ESI; Sheinis et al. 2002) at the cassegrain focus of the Keck II telescope; for B0537–286 we used the Low-Resolution Imaging Spectrometer (LRIS; Oke et al. 1995) at the cassegrain focus of Keck I. B1230–101 was observed with the newly-commissioned Magellan Inamori Kyocera Echelle spectrograph (MIKE; Bernstein et al. 2003) on the 6.5m Magellan Baade telescope.

Instrument settings were chosen for each QSO observation so as to provide coverage at the wavelengths of the redshifted Zn II and Cr II absorption lines. We achieved spectral resolutions varying between 0.14 and 0.25 \AA FWHM for the UVES and MIKE data, and of $\sim 1.16 \text{ \AA}$ and 3.87 \AA FWHM for the ESI and LRIS data respectively. These correspond to velocity resolutions of $\sim 7 \text{ km s}^{-1}$, $\sim 13 \text{ km s}^{-1}$, $\sim 48 \text{ km s}^{-1}$ and $\sim 140 \text{ km s}^{-1}$ for the UVES, MIKE, ESI and LRIS spectra respectively.

¹ We use the conventional notation whereby $[\text{Zn}/\text{H}] = \log(\text{Zn}/\text{H}) - \log(\text{Zn}/\text{H})_{\odot}$.

Table 1. Details of the QSOs observed.

QSO	B mag.	z_{em}	z_{abs}	Telescope/ Instrument	Resolution (\AA)	Integration Time (s)	S/N ^a
(1)	(2)	(3)	(4)	(5)	(6)	(7)	(8)
B0335–122	21.5 ^b	3.442	3.17995	VLT 2/UVES	0.20	16 300	7
B0347–211	20.9	2.944	1.947	VLT 2/UVES	0.14	8 900	6
B0405–331	19.4	2.570	2.56932	Keck II/ESI	1.16	3 600	15
B0432–440	19.8	2.649	2.30205	VLT 2/UVES	0.16	14 400	12
B0438–436	20.7	2.863	2.34736	VLT 2/UVES	0.16	14 700	25
B0537–286	19.8	3.110	2.9746	Keck I/LRIS	3.87	8 600	39
B0913+003	21.7 ^b	3.074	2.7434	Keck II/ESI	1.21	3 600	8
B0933–333	19.7	2.906	2.6823	VLT 2/UVES	0.18	14 400	20
B1055–301	19.4	2.523	1.90350	VLT 2/UVES	0.14	10 800	15
B1228–113	20.9	3.528	2.19289	VLT 2/UVES	0.15	18 000	15
B1230–101	19.7	2.394	1.93136	Magellan I/MIKE	0.25	18 000	11
B1354–107	19.0	3.006	2.50086 & 2.96682	VLT 2/UVES	0.17 0.19	14 400	21 14
B1418–064	20.4	3.689	3.44828	VLT 2/UVES	0.23	14 400	11
B2311–373	19.0	2.476	2.18210	VLT 2/UVES	0.15	10 800	25

^a Signal to noise ratio in the wavelength region encompassing the Zn II and Cr II absorption lines.

^b These two values are taken from Table 3 of Ellison et al. (2001b).

2.2. Data Reduction

Due to the differing nature of the instruments used, the spectra were not identically reduced, although the same standard steps were incorporated in each case. The reduction of the UVES data was performed with the ESO UVES data reduction pipeline, while the other spectra were reduced using standard IRAF² routines. The two-dimensional images were trimmed and the bias level subtracted using the over-scan regions. Pixel-to-pixel variations were corrected for by dividing through by a normalized flat-field of high S/N that had been produced by co-adding several flat-field exposures. Pixels which had been affected by cosmic ray hits were corrected for, where possible, and the echelle orders or single long-slit spectrum were traced. The one-dimensional spectrum was then extracted and the sky spectrum subtracted (in the case of MIKE taking into account the slit tilt, which is not perpendicular to each order and varies over the CCD).

The individual sky-subtracted spectra were then wavelength calibrated (using comparison lamp spectra typically taken immediately following and/or prior to each science frame and extracted in the same way as above, except for sky subtraction) and then corrected to a vacuum heliocentric wavelength scale. In the next step, the spectra of each object were rebinned to a common linear wavelength scale, with a bin size close to their original size and co-added, rejecting any remaining cosmic rays or bad pixels. The co-addition was performed without any weighting and the corresponding error spectra were summed in

² IRAF is distributed by the National Optical Astronomy Observatories, which are operated by the Association of Universities for Research in Astronomy, Inc., under cooperative agreement with the National Science Foundation

Table 2. Transition wavelengths and f -values used in this study.

Species	Wavelength (\AA)	f
Zn II	2026.1370	0.501
Mg I	2026.4768	0.113
Cr II	2056.2569	0.103
Cr II	2062.2361	0.0759
Zn II	2062.6604	0.246
Cr II	2066.1640	0.0512

quadrature. Gaussian fits to several emission lines from the reference lamp spectra near to the redshifted Zn II and Cr II lines were made to estimate the values of the spectral resolution (FWHM) listed in Table 1.

2.3. Spectral Line Fitting

Metal absorption lines associated with the DLA systems in each QSO spectrum were initially identified based on the redshifts reported by Ellison et al. (2001b). The vacuum-heliocentric wavelengths measured from our spectra for the strongest component in each absorption system were then used to determine a more accurate redshift for the DLA system, based on the average of the redshifts calculated from each (non-saturated) line. The spectra were then reduced to a rest-frame wavelength scale and cut into sections corresponding to $\pm 2000 \text{ km s}^{-1}$ around each absorption line. These sections were then normalised to the local continuum by division by a spline fit to portions of the spectrum judged to be free of absorption.

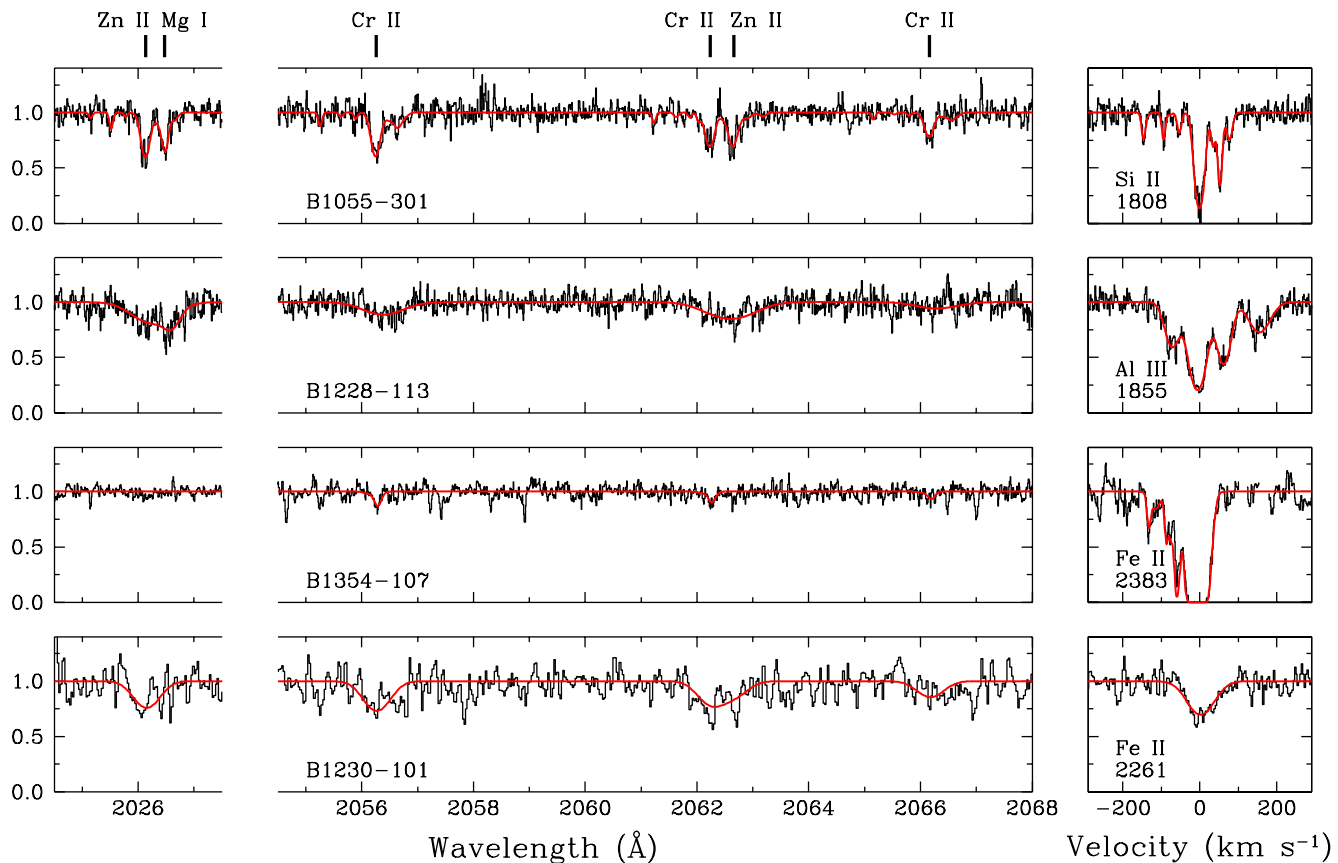


Fig. 1. Sample portions of spectra of CORALS QSOs, showing the Zn II $\lambda 2026.14$ and Mg I $\lambda 2026.48$ lines (*left*), and the Cr II $\lambda\lambda 2056.26$, 2062.24 , 2066.16 and Zn II $\lambda 2062.66$ lines (*centre*) in four DLAs. In the $z_{\text{abs}} = 2.50086$ DLA in the spectrum of B1354–107 (third panel), we just detect Cr II $\lambda\lambda 2056.26$, 2062.24 , while the other lines are below our detection limit. In the far right panels we have reproduced examples of stronger transitions from other elements which were used to determine the velocity structure of the gas in each DLA. The continuous coloured lines show the profile fits to the data produced by VPFIT (see text).

Ion column densities were deduced from the observed absorption lines using the line fitting software package VPFIT³. VPFIT fits multiple Voigt profiles (convolved with the instrument profile) to absorption line components. Initial guesses for the column density, redshift and Doppler b parameter for each absorption component are used as inputs into the program. VPFIT then computes the χ^2 goodness-of-fit (taking into account the error on each pixel) and automatically varies the parameters, iterating until χ^2 has been minimised and the best fit has been found. Components were rejected from the fit if their Doppler parameters were lower than approximately half the spectral resolution. For the rest-frame wavelengths and f -values of the transitions, which are inputs to VPFIT, we consulted the recent compilation by Morton (2003); for reference, values for the Zn II and Cr II multiplets are reproduced in Table 2.

The first step in the line fitting procedure was to determine the multi-component velocity structure of gas in the damped system by fitting lines spanning a wide range of f -

values, preferably multiplets of Fe II and Si II. The parameters of the fit—that is redshift and Doppler parameter—were then kept fixed and applied to the generally weaker Zn II and Cr II lines. In cases where only some of the Fe II and Si II absorption components are detected in Zn II and Cr II, the total column densities of Zn⁺ and Cr⁺ were adjusted upwards to allow for the unseen components in the same proportion as determined for Fe II and Si II. The implicit assumption is that the relative proportions of absorbers in each component are the same for all the ions considered. While in principle this may not be true, because of possible differences in the degree of dust depletion of different elements, in practice element ratios are found to be remarkably uniform between the multiple velocity components within a DLA (e.g. Prochaska 2003). The correction for unseen components amounted to less than $\sim 10\%$ of the total column density in all but two cases, B0432–440 and B0933–333, where the correction for unseen components is as much as $\sim 50\%$. Indeed, this correction for undetected components was the main reason why we used VPFIT to analyse the Zn II and Cr II absorption. In all cases considered here, the Zn II and Cr II lines

³ VPFIT is available from <http://www.ast.cam.ac.uk/~rfc/vpfit.html>

Table 3. Zn and Cr abundances in the damped Ly α systems observed.

QSO	z_{DLA}	$N(\text{H}^0)$ (10^{20}cm^{-2})	$N(\text{Zn}^+)$ (10^{12}cm^{-2})	$N(\text{Zn}^+)/N(\text{H}^0)$ (10^{-9})	$N(\text{Cr}^+)$ (10^{12}cm^{-2})	$N(\text{Cr}^+)/N(\text{H}^0)$ (10^{-9})	$N(\text{Cr}^+)/N(\text{Zn}^+)$
(1)	(2)	(3)	(4)	(5)	(6)	(7)	(8)
B0335–122	3.17995	6.0 ± 1.5	≤ 1.8	≤ 3.0	^a	^a	...
B0347–211	1.947	2.0 ± 0.5	≤ 2.4	≤ 12	≤ 7.4	≤ 37	...
B0405–331	2.56932	4 ± 1	≤ 5.5	≤ 14	≤ 21	≤ 54	...
B0432–440	2.30205	6.0 ± 1.5	≤ 1.6	≤ 2.7	13 ± 2	22 ± 6	≥ 8.4
B0438–436	2.34736	6.0 ± 1.5	5.3 ± 0.3	8.8 ± 2.3	12 ± 1.4	19 ± 5	2.2 ± 0.3
B0537–286	2.9746	2.0 ± 0.5	≤ 3.4	≤ 17	≤ 20	≤ 100	...
B0913+003	2.7434	5.5 ± 1.4	≤ 6.6	≤ 12	≤ 29	≤ 53	...
B0933–333	2.6823	3.0 ± 0.8	≤ 0.98	≤ 3.3	≤ 8.7	≤ 29	...
B1055–301	1.90350	35 ± 9	8.2 ± 0.5	2.3 ± 0.6	41 ± 2	12 ± 3	5.0 ± 0.4
B1228–113	2.19289	4 ± 1	10.3 ± 0.8	26 ± 7	28 ± 2	69 ± 18	2.7 ± 0.3
B1230–101	1.93136	3.0 ± 0.8	8.7 ± 1.0	29 ± 8	47 ± 4	160 ± 40	5.4 ± 0.8
B1354–107	2.50086	2.5 ± 0.6	≤ 0.5	≤ 2	7.4 ± 0.8	29 ± 8	≥ 15
B1354–107	2.96682	6.0 ± 1.5	≤ 0.85	≤ 1.4	≤ 6.0	≤ 10	...
B1418–064	3.44828	2.5 ± 0.6	≤ 0.96	≤ 3.9	≤ 5.1	≤ 20	...
B2311–373	2.18210	3.0 ± 0.8	≤ 0.66	≤ 2.2	≤ 3.4	≤ 11	...

^a The Cr II lines were not covered by the UVES observations of this QSO as they fell in the wavelength gap between the two red-arm CCDs .

Table 4. Velocity dispersion parameters of the strongest component of detected Zn II and Cr II lines

QSO	z_{DLA}	b (km s^{-1})
B0432–440	2.30205	12
B0438–436	2.34736	8
B1055–301	1.90350	16
B1228–113	2.19289	73
B1230–101	1.93136	47
B1354–107	2.50086	12

are unsaturated and we would have obtained the same values of $N(\text{Zn}^+)$ and $N(\text{Cr}^+)$ —apart from the ‘incompleteness’ correction—had we analysed them with the optical depth method (Hobbs 1974) which some prefer to profile fitting.

Out of the 15 DLAs listed in Table 1, we report positive detections of both the Zn II and Cr II multiplets in four cases (see Table 3). In two additional cases we detect Cr II but not Zn II, while in the remaining nine DLAs we place upper limits to both $N(\text{Zn}^+)$ and $N(\text{Cr}^+)$. The upper limits are 3σ , deduced from the measured S/N ratios (listed in column (8) of Table 1) and the velocity spread of the absorption implied by stronger lines of Fe II and Si II, as explained above.

Figure 1 shows examples of the spectra in the regions of the Zn II and Cr II multiplets, including three of the Zn II and Cr II detections and one case when only Cr II is

detected.⁴ Also shown in the figure are examples of the stronger lines used to determine the velocity structure of each DLA, as well as the fits generated by VPFIT. Table 4 lists values of the Doppler b parameter for the detected Zn II and Cr II lines; full details of the velocity structure of other absorption lines will be presented in a future publication (Akerman 2005).

3. Abundance determinations

Table 3 lists the column densities of Zn II and Cr II, or upper limits, measured in this study together with the 1σ uncertainties in their values. Since the first ions are the dominant ionization stages of Zn and Cr in HI regions, we can readily derive the abundances of these two elements by dividing the values of $N(\text{Zn}^+)$ and $N(\text{Cr}^+)$ by the neutral hydrogen column densities $N(\text{H}^0)$ listed in column (3) of Table 3—the results are given in columns (5) and (7) respectively. The values of $N(\text{H}^0)$ are reproduced directly from the compilation by Ellison et al. (2001b) because (a) few of our spectra include the Ly α absorption line and (b) even in cases where we cover the transition, the intermediate resolution spectra of Ellison et al. are better suited than ours to the determination of $N(\text{H}^0)$ by fitting the damping wings of the Ly α absorption line. We have adopted throughout a conservative error of $\pm 25\%$ to $N(\text{H}^0)$, based on the typical accuracy with which such measurements have been reported in the literature.

⁴ Spectra of all the CORALS QSOs covered in the present study are available from <ftp://ftp.ast.cam.ac.uk/pub/papers/CORALS/>

Table 5. Abundances in the CORALS DLA survey. Measurements are given in logarithmic units relative to the solar abundances from Lodders (2003): $12 + \log(\text{Zn}/\text{H}) = 4.63$, $12 + \log(\text{Cr}/\text{H}) = 5.65$, $12 + \log(\text{Fe}/\text{H}) = 7.47$, $12 + \log(\text{Si}/\text{H}) = 7.54$.

QSO	z_{abs}	$N(\text{H}^0)$ (10^{20}cm^{-2})	[Zn/H]	[Cr/H]	[Fe/H]	[Si/H]	Ref.
B0335–122	3.17995	6.0	≤ -1.16	...	-2.61	-2.56	
B0347–211	1.947	2.0	≤ -0.54	≤ -1.08	≤ -1.16	...	
B0405–331	2.56932	4.0	≤ -0.49	≤ -0.92	-1.74	-1.40	
B0432–440	2.30205	6.0	≤ -1.21	-1.30	-1.45	-1.12	
B0438–436	2.34736	6.0	-0.68	-1.36	-1.30	...	
B0458–020	2.0395	44.7	-1.15	-1.50	-1.61	≥ -2.10	1, 2
B0528–250	2.141	8.9	-1.45	-1.50	-1.57	-1.27	3, 4
B0528–250	2.811	12.9	-0.47	-1.11	-1.11	-0.64	3, 4
B0537–286	2.9746	2.0	≤ -0.40	≤ -0.65	
B0913+003	2.7434	5.5	≤ -0.55	≤ -0.92	-1.59	-1.47	
B0933–333	2.6823	3.0	≤ -1.12	≤ -1.19	-1.54	-1.22	
B1055–301	1.90350	35.0	-1.26	-1.58	-1.57	-1.13	
B1228–113	2.19289	4.0	-0.22	-0.81	
B1230–101	1.93136	3.0	-0.17	-0.45	-0.63	-0.24	
B1354–107	2.50086	2.5	≤ -1.32	-1.18	-1.25	...	
B1354–107	2.96682	6.0	≤ -1.48	≤ -1.65	-1.54	-1.31	
B1418–064	3.44828	2.5	≤ -1.04	≤ -1.34	-1.72	-1.48	
B2311–373	2.18210	3.0	≤ -1.29	≤ -1.60	-1.70	-1.52	
B2314–409	1.8573	7.9	-1.01	-1.17	-1.29	-1.03	5
B2314–409	1.8745	1.3	≤ -1.18	≤ -1.59	-1.85	-1.86	5

References: 1 - Prochaska & Wolfe (1999), 2 - Prochaska et al. (2001), 3 - Centurion et al. (2003), 4 - Lu et al. (1996), 5 - Ellison & Lopez (2001a).

In Table 5 we list the abundances of Zn, Cr, Fe, and Si, expressed in logarithmic units relative to solar, for each of the DLAs in the complete CORALS sample; the list includes all the new measurements reported here plus the five already available from the literature—references are given in the last column of Table 5. The only DLAs in the compilation by Ellison et al. (2001b) which are missing from our sample are the two systems in front of the very faint QSO B1251–407, as explained in §2. We have adopted throughout the solar abundances proposed by Lodders (2003) in her comprehensive reassessment of meteoritic and photospheric abundances; those from the more recent compilation by Asplund, Grevesse, & Sauval (2004) differ by no more than 0.03 dex for the elements of interest here. All the Zn and Cr measurements collected in Table 5 (and indeed those of the larger comparison sample discussed in §4) have been reduced to the same set of f -values, as listed in Table 2, except for cases where the differences in column density would have amounted to less than a few percent.⁵ It was not possible, however, to ensure the same degree of homogeneity for the Fe II and Si II measurements.

⁵ Most recent work has used the same set of f -values for the Zn II and Cr II multiplets, from the laboratory measurements by Bergeson & Lawler (1993). Small differences between the values quoted by different observers result from rounding errors.

4. Metallicity and dust in the CORALS survey

The purpose of this study is to test whether element abundances in CORALS DLAs are significantly different from those of DLAs drawn from optically selected QSO samples, and therefore to determine the extent, if any, to which previous surveys have been biased against metal-rich, high column density absorbers. We consider this question from two points of view, by examining first the metallicity distributions indicated by the [Zn/H] determinations, and then the degree of depletion of refractory elements implied by the [Cr/Zn] measures.

4.1. Comparison of Zn Abundances

The most extensive, homogeneous, compilation of [Zn/H] measurements in DLAs has recently been assembled by Kulkarni et al. (2005); it includes 51 detections and 36 upper limits over the redshift interval $z_{\text{abs}} = 0.09$ to 3.90. (Three of the Zn II detections in the Kulkarni et al. data set are in common with the CORALS survey and have thus not been included in the control sample in the following analysis.) Although larger compilations of DLA abundance measurements have been published (e.g. Prochaska et al. 2003), they bring together data for other elements, mostly Si and Fe, in addition to Zn. The improved statistics afforded by such compilations are offset, in our view, by systematic uncertainties due to differing degrees of dust depletion and possible nucleosynthetic departures from so-

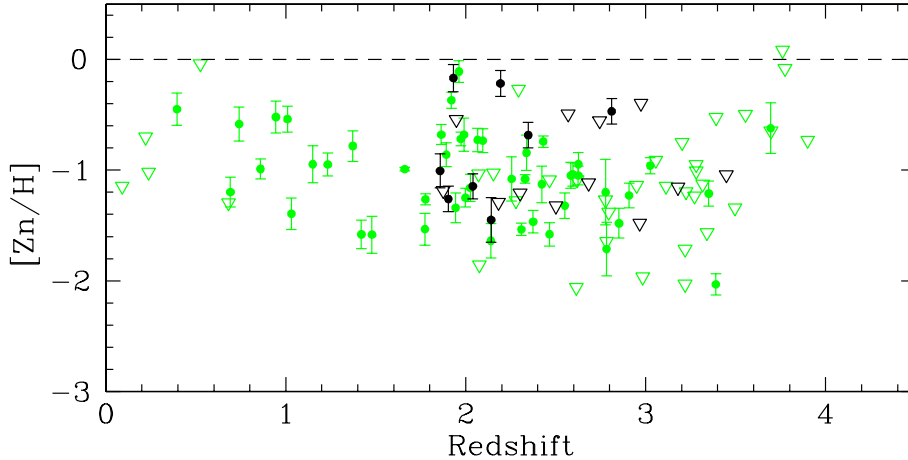


Fig. 2. Comparison of the abundance of Zn measured in DLAs in the CORALS sample (black) and in the control sample by Kulkarni et al. 2005 (coloured). Upper limits, corresponding to non-detections of the Zn II doublet, are indicated by open triangles. The abundance of Zn is plotted on a logarithmic scale relative to the solar value shown by the broken line at $[Zn/H] = 0.0$.

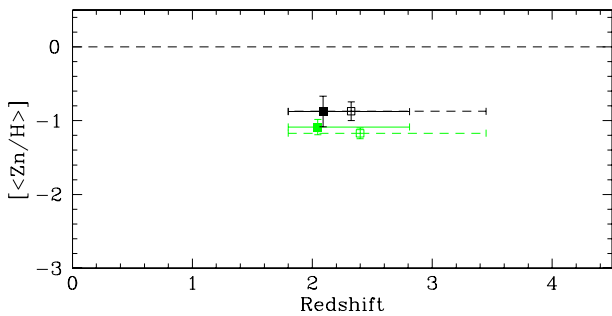


Fig. 3. Column density-weighted metallicities of DLAs in the CORALS (black) and Kulkarni et al. 2005 (coloured) samples. For each sample we show two values of $\langle [Zn/H] \rangle$; the solid squares correspond to the values obtained by considering only Zn II detections, while the open squares (and dashed error bars) are obtained if the upper limits to $[Zn/H]$ in Figure 2 are included as if they were detections. The squares are plotted at the median redshift of the DLAs in each sample.

lar relative abundances of different elements. Thus, we consider it more appropriate to restrict the present analysis to the comparison of Zn abundances alone.

The CORALS $[Zn/H]$ abundances are compared with those from the compilation by Kulkarni et al. (2005) in Figure 2 (after rescaling the latter to the solar value from Lodders 2003). From a visual inspection of the plot we conclude that: (a) both the CORALS and the comparison sample of optically selected DLAs are generally metal-poor, with typical values of $[Zn/H]$ well below solar; and (b) there is a hint that, overall, the CORALS DLAs may have marginally higher metallicities, although the consid-

erable number of upper limits complicates the comparison. We now address these points quantitatively.

The quantity which is of interest for ‘cosmic’ chemical evolution models (Pei & Fall 1995) is the column density-weighted metallicity

$$\langle [Zn/H]_{DLA} \rangle = \log \langle (Zn/H)_{DLA} \rangle - \log (Zn/H)_{\odot} \quad (1)$$

where

$$\langle (Zn/H)_{DLA} \rangle = \frac{\sum_{i=1}^n N(Zn^+)_{i}}{\sum_{i=1}^n N(H^0)_{i}} \quad (2)$$

which is a measure of the degree of metal enrichment of the DLA population as a whole. The summation in eq. (2) is over the n DLAs considered in a given sample. The present sample is too small to consider subsets of the data within different redshift intervals, as done by Pettini et al. (1999), Prochaska et al. (2003), and Kulkarni et al. (2005). Instead we compute eq. (2) for the CORALS sample as a whole, and compare the result with the analogous quantity for the Kulkarni et al. (2005) sample, *computed over the same redshift interval spanned by the CORALS data*, $z_{abs} = 1.86 - 3.45$ for the full set (57 DLAs), and $z_{abs} = 1.86 - 2.81$ for the Zn II detections only (27 DLAs). We find $\langle [Zn/H]_{DLA} \rangle = -0.88 \pm 0.21$ for CORALS DLAs, and $\langle [Zn/H]_{DLA} \rangle = -1.09 \pm 0.10$ for the control sample of Kulkarni et al. (2005). These values, which differ at only the 1σ level, were calculated considering only the Zn II detections. Repeating the calculations, but now including the upper limits as if they were detections, we obtain $\langle [Zn/H]_{DLA} \rangle = -0.87 \pm 0.13$ and -1.17 ± 0.07 respectively. The errors were estimated using bootstrap techniques (Efron & Tibshirani 1993). For

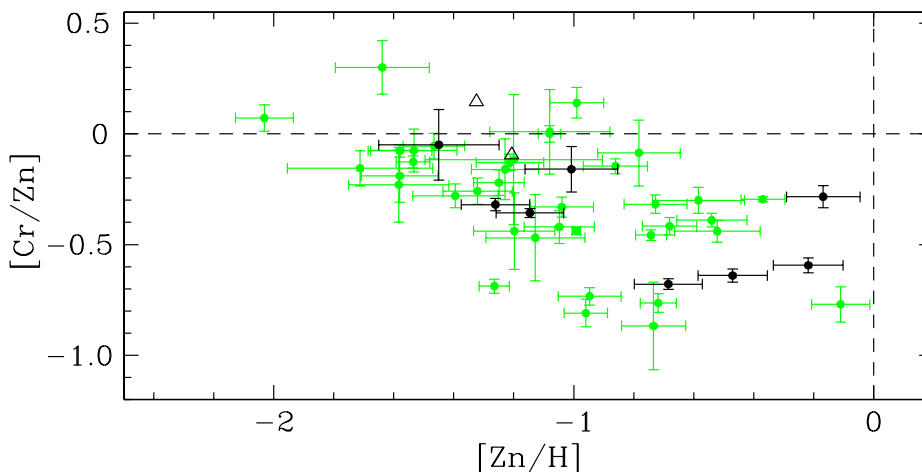


Fig. 4. Cr/Zn ratio against Zn abundance for CORALS DLAs (black) and DLAs from the compilation by Kulkarni et al. (2005; coloured). Lower limits, corresponding to cases where Cr II lines are detected by Zn II lines are not, are indicated by open triangles. Abundance ratios are plotted in logarithmic units relative to the solar values shown by the broken lines at $[\text{Cr}/\text{Zn}] = 0.0$ and $[\text{Zn}/\text{H}] = 0.0$.

each sample (CORALS and the control sample), we constructed random datasets by drawing n times from the real dataset with replacement, where n is the number of $[\text{Zn}/\text{H}]$ measurements in each sample. The procedure was repeated a million times to build up a distribution of values of $\{[(\text{Zn}/\text{H})_{\text{DLA}}]\}$; we quote the standard deviation of this distribution as our estimate of the error in the quantity $\{[(\text{Zn}/\text{H})_{\text{DLA}}]\}$.

These results are shown graphically in Figure 3. Again we see that the two samples are very similar. The marginally higher metallicity of the CORALS sample may be real. Alternatively it may be an artifact of small number statistics or, in the case where we include upper limits, it may be due to the higher proportion of upper limits skewing the results—over one half of the CORALS measures of $[\text{Zn}/\text{H}]$ are upper limits, compared with one third for the control sample of Kulkarni et al. (2005).

In order to clarify this point, we conducted a statistical test based on “survival statistics” (which takes account of upper limits) with the program ASURV (LaValley, Isobe & Feigelson 1992), which implements the statistical methods of Feigelson & Nelson (1985). Using a Peto-Prentice test (Latta 1981), we tested the null hypothesis that the two samples are drawn from the same parent population and found the hypothesis to be true at the 90% confidence level. We conclude that CORALS DLAs do not exhibit significantly different metallicities from those of existing, larger, samples of DLAs assembled from optically selected QSO surveys.

4.2. Comparison of Cr/Zn ratios

An indication of the degree of depletion of refractory elements onto dust grains may be obtained from the ratio of the abundances of chromium to zinc, as explained in §1. In

Figure 4 we plot this ratio against the metallicity $[\text{Zn}/\text{H}]$ for each of the CORALS DLAs (coloured) from Table 5 together with analogous measurements (black) from the compilations by Khare et al. (2004) and Kulkarni et al. (2005), after rescaling their values to the same solar abundances used here.

Figure 4 shows the trend of increasing Cr depletion with increasing metallicity which was previously noted by Pettini et al. (1997a) and shown by Prochaska & Wolfe (2002) to be a general feature of refractory elements in DLAs. In systems with $[\text{Zn}/\text{H}] \lesssim -1.5$, $[\text{Cr}/\text{Zn}]$ is approximately solar—indicating that there is little dust depletion at such low metallicities—while when $[\text{Zn}/\text{H}] > 1$, up to $\sim 90\%$ of the Cr can be ‘missing’ from the gas phase and presumably be in solid form. Even so, in none of the DLAs do we see the extreme depletions of Cr, by two orders of magnitude, commonly measured in cold clouds of the Milky Way disk (Savage & Sembach 1996). At the typical DLA metallicity, $\{[(\text{Zn}/\text{H})_{\text{DLA}}]\} \approx -1$, approximately 1/2 to 2/3 of the Cr is in the dust ($[\text{Cr}/\text{Zn}] \approx -0.3$ to -0.5) although there is considerable dispersion in the depleted fraction f_{Cr} .

All of these facets of the depletion of refractory elements in DLAs have recently been discussed by Vladilo (2004) who linked them to the (generally early) chemical evolution of the galaxies where the absorption systems originate. The dependence of f_{Cr} on $[\text{Zn}/\text{H}]$ may reflect a metallicity dependence of the efficiency of dust formation in the ejecta of core-collapse supernovae and in the winds of late-type giants. On the other hand, the large scatter which accompanies the overall trend is presumably an indication of how the detailed balance between the processes of dust formation, accretion, and destruction is affected by the local physical conditions in the ISM.

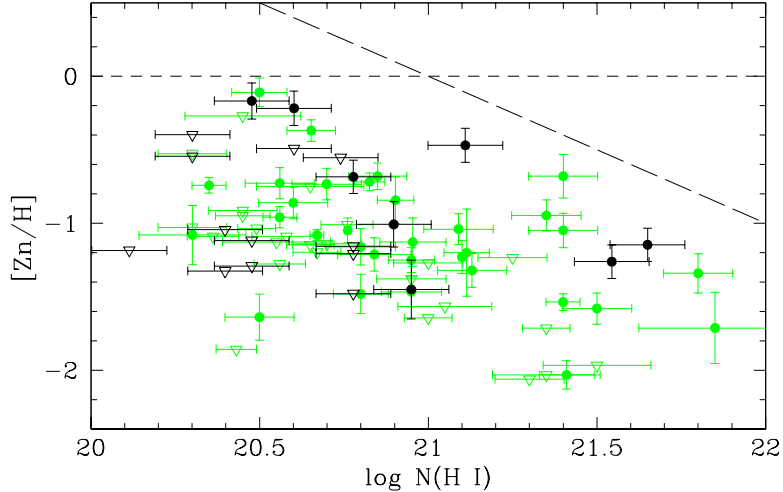


Fig. 5. Zn abundance vs. H I column density for the 20 CORALS DLAs (black) and the 57 DLAs from the compilation by Kulkarni et al. (2005; coloured) in the redshift range $1.86 \leq z \leq 3.45$. Symbols have the same meaning as in Figure 2. The long-dash line indicates the limit $[\text{Zn}/\text{H}] + \log N(\text{H I}) > 21$ beyond which Prantzos & Boissier (2000) noted that there are no DLAs. This limit seems to apply to CORALS DLAs too, although it could just be a reflection of the small size of our current sample (DLAs with $\log N(\text{H I}) > 21$ are rare). Alternatively, there may be reasons other than dust-induced bias to explain this apparent ‘zone of avoidance’. Possibly, the cross-section for high $N(\text{H I})$ absorption decreases with increasing metallicity as gas is consumed by star formation.

As far as the present work is concerned, it is evident from Figure 4 that the depletions of Cr in the CORALS sample conform to the overall pattern described above. The CORALS DLAs are not extreme in their values of f_{Cr} , nor do they exhibit lower values of $[\text{Cr}/\text{Zn}]$ at a given $[\text{Zn}/\text{H}]$ than DLAs drawn from optically selected QSO samples.⁶ If there are any DLAs where the depletions of refractory elements approach the high values typical of cold clouds in the Milky Way disk, we have not found them yet. Based on the data in Figure 4, there is no evidence that CORALS DLAs should redden the spectra of background QSOs any more than a typical DLA from an optically selected sample.

5. Discussion

The work described in this paper concludes a project begun six years ago to test the extent to which existing DLA samples are biased by dust reddening against gas-rich galaxies of high metallicity. The first results, reported by Ellison et al. (2001), showed that Ω_{DLA} had not been significantly underestimated. To that conclusion we now add the findings that:

(1) At redshifts $1.9 < z < 3.5$, the metallicity of CORALS DLAs, as measured by the $[\text{Zn}/\text{H}]$ ratio, is only marginally higher (at a statistically *insignificant* level of

⁶ Although three out of the four CORALS DLAs with $[\text{Zn}/\text{H}] < -1.0$ have $[\text{Cr}/\text{Zn}] < -0.5$ compared to only five out of 16 from the control sample, these two fractions are different at less than the 1σ significance level even when using Poisson statistics (which overestimate the significance of any differences between samples when the number of measurements is so small).

only 1σ) than that of DLAs drawn from optically selected QSOs—we determine $[\langle (\text{Zn}/\text{H})_{\text{DLA}} \rangle] = -0.88 \pm 0.21$ for CORALS DLAs, and $[\langle (\text{Zn}/\text{H})_{\text{DLA}} \rangle] = -1.09 \pm 0.10$ for the control sample of Kulkarni et al. (2005) over the same redshift interval. We note that none of the CORALS DLAs lie in the dust-‘forbidden’ zone of Prantzos & Boissier (2000) where $[\text{Zn}/\text{H}] + \log N(\text{H I}) > 21$ (see Figure 5).

(2) The dust-to-metals ratio, as measured by the quantity $[\text{Cr}/\text{Zn}]$, exhibits no systematic difference between the two samples—we unearthed no evidence to show that radio-selected QSOs should be more reddened by intervening systems than optically selected QSOs.

These results, together with recent reports of low dust extinction in large DLA samples drawn from the Sloan Digital Sky Survey (e.g. Murphy & Liske 2004), make it increasingly difficult to appeal to dust-induced selection effects to explain the observed properties of DLAs. It seems unlikely, for example, that the true metallicity of DLAs may have been underestimated by as much as a factor of five, as recently claimed by Vladilo & Péroux (2005). Below the redshift limit of our sample, $z < 1.8$, the situation is less clear. The dust fraction may be higher (e.g. Vladilo 2004), but the number density of Mg II absorbers from an extension of the CORALS radio-selected sample (in the range $0.6 < z < 1.7$) is in excellent agreement with that from optically selected surveys (Ellison 2005), suggesting that dust obscuration is not a problem at these lower redshifts either.

One caveat (often mentioned when considering the results of the CORALS survey) is the limited size of the CORALS DLA sample: are the 20 DLAs in Table 5 representative of the population as a whole, or are we being thrown off course by a statistical fluctuation? Clearly, only

future observations of a larger sample of radio selected (or possibly X-ray selected) QSOs will settle this issue and test, for instance, whether the higher metallicity—by 0.21 dex—reported here is a real difference, or possibly even an underestimate of the true value of $[\langle(\text{Zn}/\text{H})_{\text{DLA}}\rangle]$ in an unbiased sample of DLAs. For the moment, in the absence of better statistics, we can use a Monte-Carlo approach to address such concerns, particularly if we wish to test for differences at a level as high as the factor of five claimed by Vladilo & Péroux (2005).

Specifically, we have investigated the likelihood of measuring a column density weighted metallicity $[\langle(\text{Zn}/\text{H})_{\text{DLA}}\rangle] \leq -0.88$, as found here, by drawing 20 DLAs at random from a much larger parent sample of DLAs with the column density and metallicity distributions proposed by Vladilo & Péroux (2005). These authors approximated the true HI column density distribution with a power law of the form $f_{N(\text{HI})} \propto N(\text{HI})^{-\beta}$, and the true metallicity distribution with a Schechter function $f_Z \propto (Z/Z_*)^\alpha e^{-Z/Z_*}$ (motivated by luminosity-metallicity relationship of galaxies in the local universe). The least extreme set of parameters among those considered by Vladilo & Péroux has $\beta = 1.6$, $\alpha = -0.46$ and $\log(Z_*/Z_\odot) = -0.19$; with these values, their column density weighted metallicity is $[\langle(\text{Zn}/\text{H})_{\text{DLA}}\rangle] = -0.44$. Our simulations showed that, drawing 20 DLAs at random from this parent population, one would find by chance values of $[\langle(\text{Zn}/\text{H})_{\text{DLA}}\rangle]$ as low as -0.88 , or lower, only in five cases out of a hundred.

The absence of a detectable dust-related bias in current magnitude-limited samples of optically selected QSOs may appear surprising to some. After all, such a bias has long been advocated by theorists to improve the match of their models to the properties of DLAs (e.g. Cen et al. 2003; Churches et al. 2004; Nagamine et al. 2004). It also seemed the natural explanation for the empirical lack of DLAs with high column densities of metals highlighted by Boissé et al. (1998) and still present in the larger sample assembled by Kulkarni et al. (2005) and indeed in the CORALS sample considered here (see Figure 5). The reason why most optical QSO samples do not underestimate significantly quantities such as Ω_{DLA} and Z_{DLA} compared with CORALS was clarified by Ellison et al. (2004) and is related to the shape of the QSO luminosity function. Optical QSO surveys will not yield significantly skewed DLA statistics provided they reach below the break in the QSO luminosity function at $B \sim 19$. Brighter QSO samples, on the other hand, may show a bias from either dust extinction or lensing (the two effects would of course operate in different directions).

The main conclusion of the CORALS project so far—that there are only minor differences, if any, between DLA samples drawn from QSOs surveys at radio and at optical wavelengths—can only be regarded as ‘good news’. Its corollary is that the large data samples being made available by major projects such as the Two-degree Field and the Sloan Digital Sky Survey afford us an unfettered view of the absorber population, although surveys which con-

centrate only on bright QSOs may not. The challenge is now to understand, perhaps with more focused theoretical efforts, the rightful place of damped Ly α systems within the diverse population of galaxies known to inhabit the high redshift universe.

Acknowledgements. We are very grateful to Varsha Kulkarni for providing us with her compilation of Zn and Cr measurements, to Kurt Adelberger and Naveen Reddy for their assistance with the Keck observations, and to the anonymous referee whose suggestions improved the paper. We also acknowledge useful discussions with Giovanni Vladilo. We wish to recognize the significant cultural role and reverence that the summit of Mauna Kea has always had within the indigenous Hawaiian community. We are most fortunate to have the opportunity to conduct observations from this mountain.

References

- Akerman, C. J. 2005, in preparation
- Asplund, M., Grevesse, N., & Sauval, J. 2004, in Cosmic abundances as records of stellar evolution and nucleosynthesis, eds. F. N. Bash & T. G. Barnes, ASP conf. series, in press (astro-ph/0410214)
- Bergeson, S. D. & Lawler J. E. 1993, ApJ, 408, 382
- Bernstein, R., Shethman, S. A., Gunnels, S. M., Mochnacki, S., & Athey, A. E. 2003, SPIE, 4841, 1694
- Boissé, P., Le Brun, V., Bergeron, J., & Deharveng, J. 1998, A&A, 333, 841
- Boissier, S., Péroux, C., & Pettini, M. 2003, MNRAS, 338, 131
- Bresolin, F., Garnett, D. R., & Kennicutt, R. C. 2004, ApJ, 615, 228
- Cayrel, R., et al. 2004, A&A, 416, 1117
- Cen, R., Ostriker, J. P., Prochaska, J. X., & Wolfe, A. M. 2003, ApJ, 598, 741
- Centurión, M., Molaro, P., Vladilo, G., Péroux, C., Levshakov, S. A., & D’Odorico, V. 2003, A&A, 403, 55
- Chen, H., & Lanzetta, K. M. 2003, ApJ, 597, 706
- Chen, H., Kennicutt, R. C., & Rauch, M. 2005, ApJ, 620, 703
- Chen, Y. Q., Nissen, P. E., & Zhao, G. 2004, A&A, 425, 697
- Christensen, L., Schulte-Ladbeck, R. E., Sánchez, S. F., Becker, T., Jahnke, K., Kelz, A., Roth, M. M., & Wisotzki, L. 2005, A&A, 429, 477
- Churches, D. K., Nelson, A. H., & Edmunds, M. G. 2004, MNRAS, 347, 1234
- Dekker, H., D’Odorico, S., Kaufer, A., Delabre, B., & Kotzlowski, H. 2000, in SPIE Proc. 4008, 534
- de Mello, D. F., Daddi, E., Renzini, A., Cimatti, A., di Serego Alighieri, S., Pozzetti, L., & Zamorani, G. 2004, ApJ, 608, L29
- Efron, B. & Tibshirani, R. J. 1993, An Introduction to the Bootstrap (New York: Chapman & Hall)
- Ellison, S. L. 2005, Proceedings of IAUC 199: Probing Galaxies through Quasar Absorption Lines, eds. P. R. Williams, C. Shu, and B. Menard, in press (astro-ph/0505111)
- Ellison, S. L., Churchill, C. W., Rix, S. A., & Pettini, M. 2004, ApJ, 615, 118
- Ellison, S. L., Hall, P. B., & Lira, P. 2005a, AJ, submitted
- Ellison, S. L., Kewley, L. J., & Mallén-Ornelas, G. 2005b, MNRAS, 357, 354
- Ellison, S. L. & Lopez, S. 2001a, A&A, 380, 117
- Ellison, S. L., Yan, L., Hook, I. M., Pettini, M., Wall, J. V., & Shaver, P. 2001b, A&A, 379, 292

- Fall, S. M. & Pei, Y. C. 1993, *ApJ*, 402, 479
- Feigelson, E. D., & Nelson, P. I. 1985, *ApJ*, 293, 192
- Heisler, J., & Ostriker, J. P. 1988, *ApJ*, 332, 543
- Hobbs, L. M. 1974, *ApJ*, 191, 381
- Hook, I. M., Shaver, P. A., Jackson, C. A., Wall, J. V., & Kellermann, K. I. 2003, *A&A*, 399, 469
- Jackson, C. A., Wall, J. V., Shaver, P. A., Kellermann, K. I., Hook, I. M., & Hawkins, M. R. S. 2002, *A&A*, 386, 97
- Khare, P., Kulkarni, V. P., Lauroesch, J. T., York, D. G., Crotts, A. P. S., & Nakamura, O. 2004, *ApJ*, 616, 86
- Kulkarni, V. P., Fall, S. M., Lauroesch, J. T., York, D. G., Welty, D. E., Khare, P., & Truran, J. W. 2005, *ApJ*, 618, 68
- Latta, R. B. 1981, *J. Am. Statistical Association*, 26, 713
- LaValley, M., Isobe, T., & Feigelson, E. D. 1992, "ASURV", *BAAS*, 24, 839
- Lodders, K. 2003, *ApJ*, 591, 1220
- Lu, L., Sargent, W. L. W., Barlow, T. A., Churchill, C. W., & Vogt, S. S. 1996, *ApJS*, 107, 475
- Meyer, D. M., Welty, D. E., & York, D. G. 1989, *ApJ*, 343, L37
- Mo, H. J., Mao, S., & White, S. D. M. 1998, *MNRAS*, 295, 319
- Morton, D. C. 2003, *ApJS*, 149, 205
- Murphy, M. T. & Liske, J. 2004, *MNRAS*, 354, L31
- Nagamine, K., Springel, V., & Hernquist, L. 2004, *MNRAS*, 348, 435
- Oke, J. B., Cohen, J. G., Carr, M., Cromer, J., Dingizian, A., & Harris, F. H. 1995, *PASP*, 107, 375
- Pei, Y. C., & Fall, S. M. 1995, *ApJ*, 454, 69
- Pei, Y. C., Fall, S. M., & Bechtold, J. 1991, *ApJ*, 378, 6
- Péroux, C., McMahon, R. G., Storrie-Lombardi, L. J., & Irwin, M. J. 2003, *MNRAS*, 346, 1103
- Pettini, M. 2004, in *Cosmochemistry. The melting pot of the elements*, eds. C. Esteban, R.J. García López, A. Herrero, & F. Sánchez, (Cambridge, Cambridge University Press), 257
- Pettini, M., Boksenberg, A., & Hunstead, R. W. 1989, *NATO ASIC Proc. 264: The Epoch of Galaxy Formation*, 107
- Pettini, M., Boksenberg, A., & Hunstead, R. W. 1990, *ApJ*, 348, 48
- Pettini, M., Ellison, S. L., Steidel, C. C., & Bowen, D.V. 1999, *ApJ*, 510, 576
- Pettini, M., King, D. L., Smith, L. J., & Hunstead, R. W. 1997a, *ApJ*, 478, 536
- Pettini, M., Rix, S. A., Steidel, C. C., Adelberger, K. L., Hunt, M. P., & Shapley, A. E. 2002, *ApJ*, 569, 742
- Pettini, M., Smith, L. J., Hunstead, R. W., & King, D. L. 1994, *ApJ*, 426, 79
- Pettini, M., Smith, L. J., King, D. L., & Hunstead, R. W. 1997b, *ApJ*, 486, 665
- Prantzos, N., & Boissier, S. 2000, *MNRAS*, 315, 82
- Prochaska, J. X. 2003, *ApJ*, 582, 49
- Prochaska, J. X., et al. 2001, *ApJS*, 137, 21
- Prochaska, J. X., Gawiser, E., Wolfe, A. M., Castro, S., & Djorgovski, S. G. 2003, *ApJ*, 595, L9
- Prochaska, J. X., & Wolfe, A. M. 1999, *ApJS*, 121, 369
- Prochaska, J. X., & Wolfe, A. M. 2000, *ApJ*, 533, L5
- Prochaska, J. X., & Wolfe, A. M. 2002, *ApJ*, 566, 68
- Rao, S. M., Nestor, D. B., Turnshek, D. A., Lane, W. M., Monier, E. M., & Bergeron, J. 2003, *ApJ*, 595, 94
- Rao, S. M. & Turnshek, D. A. 2000, *ApJS*, 130, 1
- Ryan-Weber, E. V., Webster, R. L., & Staveley-Smith, L. 2003, *MNRAS*, 343, 1195
- Savage, B. D., & Sembach, K. R. 1996, *ARA&A*, 34, 279
- Sheinis, A. I., Bolte, M., Epps, H. W., Kibrick, R. I., Miller, J. S., Radovan, M. V., Bigelow, B. C., & Sutin, B. M. 2002, *PASP*, 114, 851
- Shapley, A. E., Erb, D. K., Pettini, M., Steidel, C. C., & Adelberger, K. L. 2004, *ApJ*, 612, 108
- Storrie-Lombardi, L. J., & Wolfe, A. M. 2000, *ApJ*, 543, 552
- Stoughton, C. et al. 2002, *AJ*, 123, 485
- Swinbank, A. M., Smail, I., Chapman, S. C., Blain, A. W., Ivison, R. J., & Keel, W. C. 2005, *ApJ*, 617, 64
- Vladilo, G. 2004, *A&A*, 421, 479
- Vladilo, G., & Péroux, C. 2005, *A&A*, submitted (astro-ph/0502137)
- Weatherley, S. J., Warren, S. J., Møller, P., Fall, S. M., Fynbo, J. U., & Croom, S.M. 2005, *MNRAS*, in press (astro-ph/0501422)
- Wolfe, A. M., Lanzetta, K. M., Foltz, C. B., & Chaffee, F. H. 1995, *ApJ*, 454, 698
- Wolfe, A. M., Turnshek, D. A., Smith, H. E., & Cohen, R. D. 1986, *ApJS*, 61, 249